CrossMark

ORIGINAL PAPER

Effect of Slope Angle on Seismic Response of Unreinforced and Reinforced Soil Slopes in Shaking Table Tests

N. Srilatha[1] · G. Madhavi Latha[2] · C. G. Puttappa[3]

Abstract This paper studies the effect of slope angle on the seismic response of unreinforced and reinforced soil slopes through a series of laboratory shaking table tests. Slopes were constructed using clayey sand and geogrids were used for reinforcing the slopes. The slope angle varies from 45°, 60° and 75° in different tests and the quantity and location of reinforcement is varied in different tests. Acceleration of base shaking varies from 0.1 to 0.3 g in the model tests and the frequency of base shaking was 2–10 Hz in different tests. The slope is instrumented with ultrasonic displacement sensors and accelerometers at different elevations. The response of different slopes is compared in terms of the horizontal displacements of the slope and acceleration amplifications measured at different elevations. At all frequency levels and base acceleration conditions, unreinforced slopes showed higher acceleration amplifications and increased displacements with the increase in steepness It was also observed from the test results that increase in steepness of the slope has detrimental effects on both acceleration amplifications and displacement response of unreinforced as well as reinforced model soil slopes.

✉ G. Madhavi Latha
madhavi@civil.iisc.ernet.in

N. Srilatha
srilatha@civil.iisc.ernet.in

C. G. Puttappa
puttappacg@gmail.com

[1] Indian Institute of Science, Bangalore 560012, India

[2] Department of Civil Engineering, Indian Institute of Science, Bangalore 560012, India

[3] Department of Civil Engineering, MSRIT, Bangalore 560054, India

Introduction

Soil reinforcement using high tensile strength inclusions can increase the shearing resistance of a soil mass. The increase in strength permits the construction of soil structures at slope angles greater than the angle of repose and/or greater than would be possible without the reinforcement [1]. Physical modeling was successfully used by many researchers to investigate the collapse of granular materials and the role of different parameters related to slope, soil and fluid pressure on slope stability [2]. However, the knowledge on the seismic performance of the reinforced soil slopes under seismic conditions is not studied by many. Shaking table experiments are successfully used in earthquake engineering to simulate the seismic behaviour of structures and granular soils. Studies reported by [3–17] demonstrated the successful use of shaking table for understanding seismic response of soil structures. The present study evolved from the need for systematic studies that investigate the influence of geometry of slopes on their response to earthquake shaking, which is evident from the review of literature presented in the next section.

Background

Several laboratory model tests, numerical studies and field studies on unreinforced and reinforced soil structures subjected to seismic shaking conditions were reported by

earlier researchers. Koga et al. [18] performed shaking table tests on 1.8 m high, 1 H:3 V slopes with sand bag facing. The slopes were subjected to 40 cycles of harmonic loading with increasing amplitude. The test results showed that the permanent displacements increased with increasing input motion amplitude and decreased with increasing reinforcement stiffness, density, and decreasing slope angle. Kramer [19] described that the permanent displacements of the slope are functions of the slope angle, shear strength of the slope soil and the acceleration of the seismic event normalized with the yield acceleration, which corresponds to a factory of safety of 1.0. Makdisi and Seed [20] and Yegian et al. [21] attempt to predict the permanent deformations of slopes with respect to the ratio of yield acceleration of the slope to the maximum acceleration of the event. Perez and Holtz [22] discussed some of the shaking table tests on geosynthetic reinforced soil slopes subjected to a base shaking frequency of 5 Hz. Lo Grasso et al. [7] investigated the performance of reinforced slopes through a number of shaking table tests built with an inclination of 70° with respect to the horizontal to a height of 0.35 m. It was concluded from the study that reducing the spacing of reinforcement near the top of the model is beneficial for the stability of the slope. Presence of surcharge was found to be effective in altering the failure surface mechanism; failure mechanism was approximated to a circular surface for slopes with surcharge, while for a slope without surcharge it was a typical two-wedge mechanism. Viswanadham and Mahajan [23] performed series of centrifuge tests on wrap-around geotextile reinforced sand slopes with different slope inclinations and observed that the magnitude of peak strain at failure increases with the increase in slope inclination.

Turan et al. [24] summarized the results from series of shaking table tests and numerical analyses that were performed to study the performance of the laminar box and non-linear seismic behavior of the model clay are described and the effect of boundary on measured accelerations was found to be negligible. Krishna and Latha [25] showed that the inclusion of reinforcing material was very effective in minimizing the horizontal displacements of retaining walls. It was demonstrated that retaining walls with a very low strength geonet and geotextile can also achieve displacement reductions of 75% compared to the unreinforced wall. The acceleration amplifications varied with the type of reinforcing material but the trends were inconsistent. Ling et al. [26] showed that geocells can be used successfully to form gravity walls as well as reinforcement layers even when subjected to a very high seismic load. The results as reported should be useful for developing and validating numerical procedures in analyzing the seismic behavior of geocell reinforced soil retaining walls. Huang et al. [11]

discussed the seismic design of full scale geosynthetic-reinforced slopes through laboratory experiments. Test results indicated that both the horizontal acceleration response at the crest and the lateral slope displacement are influenced by the horizontal peak ground acceleration, wave frequency and the cumulative permanent displacement of the slope. Huang et al. [12] carried out uni-axial shaking table tests on 480 mm high geosynthetic reinforced model slopes with a slope angle of 60° to understand the influence of peak horizontal ground acceleration and wave frequencies on the seismic displacement of the slope. Investigations were also performed to obtain the relationship between the amplification response and the plastic displacement of the slope. Liu et al. [27] described three cases of failures of geosynthetic reinforced slopes occurred over a duration of 10 years in central Taiwan. Lessons learned from these case histories with regard to the importance of detailed site investigation, selection of backfill, installation of proper drainage systems and design were discussed in this study. Rajabian et al. [28] studied the behavior of unreinforced and anchored geosynthetic reinforced slopes under seepage using centrifuge tests, effect of slope inclination and number of anchors on the stability and deformation behavior of reinforced slopes was investigated. Yang et al. [29] conducted series of dynamic centrifuge tests to investigate the acceleration amplified and de-amplified responses within geosynthetic-reinforced soil (GRS) structures. This study describes the acceleration amplification characteristics of GRS structures are highly dependent on input ground acceleration, location and input motion frequency. Latha and Verman [30] simulated shaking table tests on geotextile reinforced soil slopes in the numerical model using the computer program GEO-STUDIO. In this study, the SLOPE/W and QUAKE/W modules of this program were used to construct the slopes and to apply dynamic base shaking. Soil was modeled as a Mohr–Coulomb material and geotextile was modeled as a structural beam element of flexible material with the properties obtained from laboratory experiments. The simple numerical model was able to predict the measured experimental displacements reasonably well. Dong et al. [31] carried out shaking table model studies on unreinforced soil slopes and results showed that the effect of slope geometry on the amplification of motion, location of the initiation of failure, development of the sliding surface and final shape of the failed slope. Literature review suggests that few earlier researchers had investigated the effect of slope geometry on the static and seismic response of reinforced soil slopes. This paper presents the results from shaking table tests to understand the effect of slope angle on acceleration, frequency of base shaking and reinforcement on the performance of the slope during seismic excitation.

Equipment and Materials Used in the Experiments

Shaking Table

A computer controlled servo hydraulic single degree of freedom (horizontal) shaking table facility has been used in simulating horizontal seismic action, associated with seismic or any other vibration conditions. The shaking table has a loading platform of 1 m × 1 m size and the payload capacity is 1 ton. The shaking table can be operated within the acceleration range of 0.05–2 g and frequency range of 0.05–50 Hz within the amplitude of ±200 mm. The major problems associated with laboratory model studies are scaling and the boundary effects, especially in studies related to earthquake engineering. Models of soil slopes have been built in a laminar box to reduce the boundary effect to some extent. The laminar box used for the tests is rectangular in cross section with inside dimensions of 500 mm × 1000 mm and 800 mm deep with 15 rectangular hollow aluminum layers. These layers are separated by linear roller bearings arranged to permit relative movement between the layers with minimum friction.

Soil

Locally available soil was used to prepare the model slopes. The soil is classified as clayey sand (SC) according to the Unified soil classification system. Particle size distribution of the test soil is shown in Fig. 1. The effective cohesion and friction angle of the soil are 33 kPa and 33°, respectively as determined from the consolidated undrained triaxial compression tests. The properties of the soil are listed in Table 1.
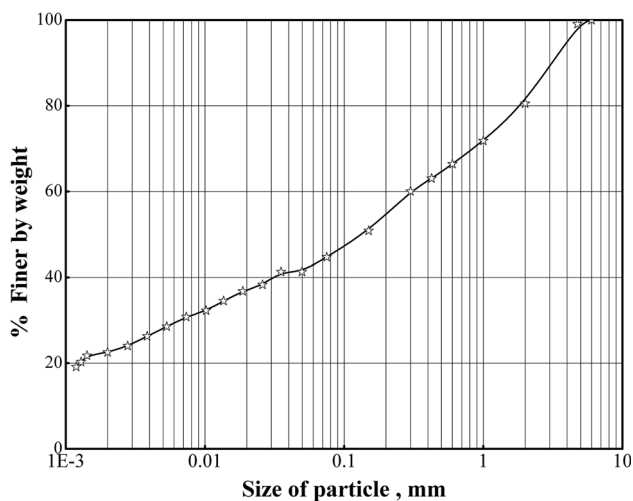
Reinforcement

A biaxial geogrid made of polypropylene is used in the present study to reinforce the soil slopes. The load- elongation response of biaxial geogrid obtained from standard multi-rib tension test as per ASTM D 6637 [32] is shown in Fig. 2. The properties of the geogrid are listed in Table 2.

Instrumentation

Accelerometers and ultrosonic non-contact displacement transducers (USDT) are used to measure the response of the model slope during shaking. Accelerometers are of analog voltage output type with a full-scale acceleration range of ±2 g along both the x and y axes, with sensitivity

Table 1 Properties of the soil

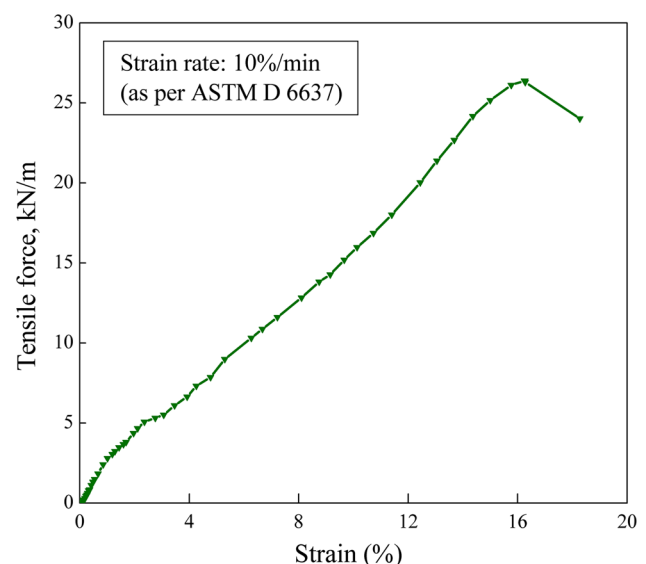| Property	Value
Specific gravity	2.67
Percentage of gravel fraction	1
Percentage of sand fraction	55
Percentage of silt fraction	21
Percentage of clay fraction	23
Soil classification	SC
Liquid limit (%)	34
Plastic limit (%)	23
Maximum dry unit weight from standard Proctor compaction test (kN/m^3)	17.67
Optimum moisture content from standard Proctor compaction test (%)	16.31

Fig. 1 Grain size distribution curve of the test soil

Fig. 2 Load-elongation response of the geogrid from multi-rib tension test

Table 2 Properties of the geogrid

Parameter	Value
Ultimate tensile strength (kN/m)	26
Yield point strain (%)	16.50
Aperture size	35 mm × 35 mm
Aperture shape	Square
Stiffness at 5% strain (kN/m)	125
Mass per unit area (kg/m^2)	0.22

of 0.001 g and these accelerometers are connected to the shaking table controller through junction box for data acquisition. Non contact type ultrasonic displacement transducers are used to measure the horizontal displacements at different elevations. These sensors work on ultrasonic energy multiple pulses, which travel through the air at the same speed of sound. The sensing range of these sensors is 30–300 mm with short dead zone of 30 mm and output response time is 30 ms.

Model Construction and Testing Methodology

To minimize the friction between the model and the laminar box, polyethylene sheet was used inside of the laminar box and also to cover the gap between the each rectangular panel. For compaction, a mass of 5 kg was dropped from a height of 450 mm on 150 mm × 150 mm square steel base plate with fixed guide rod at the centre of the base plate to achieve the desired unit weight for each layer. Three layered compaction was adopted for unreinforced and two layer reinforced slopes and four layered compaction was used for one layer and three layer reinforced slopes. Reinforcement was placed at the interface of the compacted soil layers. Each model is constructed using clayey sand, compacted in three equal lifts, each of 200 mm, to get a total slope height (H) of 600 mm with a base width of 850 mm. The remaining space in the laminar box (150 mm × 500 mm in plan) was kept empty for mounting the displacement transducers and that space was packed

with concrete cubes enclosed in plywood panels during compaction. Then the slope of required angle is marked and carefully cut using a trowel. The unit weight and water content of the slopes were kept as 15 kN/m^3 and 10%, respectively in all the model tests. The geogrid reinforcement is provided at the interface of the compacted layers and is kept at a distance of 50 mm from the face of the slope to the full width of the slope for all the reinforced model slopes. The compacted soil was trimmed to the required slope geometry. After finishing the model preparation the plywood and concrete cubes were removed one by one. During the process of compaction the accelerometers, A1, A2 and A3 were embedded in soil at elevations 170, 370 and 570 mm from the base of the slope, where one accelerometer, A0, was fixed rigidly to the bottom of the shaking table to measure base acceleration. Three displacement transducers, U1, U2 and U3 were positioned along the face of the slope at elevations 200, 350 and 500 mm from the base of the slope to measure the horizontal face displacements. The transducers are fitted in wooden planks which were bolted horizontally to the T-shape steel bracket which is in turn fitted to the steel frame. Schematic diagram of typical slopes of different slope angles with instrumentation is as shown in Fig. 3. The response of the slope was recorded in terms of acceleration at different elevations and the displacement of the facing. Shaking table tests in this study are 1 g model studies carried out on reduced scale models. The stresses and deformations measured in the experiments do not truly represent the stresses and deformations in field because of low confining pressures and boundary effects in model studies. Hence it is essential to apply proper similitude rules for the experiments in order to apply the results to actual field conditions. Iai [33] presented similitude laws for the 1 g model tests from basic definitions of effective stress, strain and constitutive law, overall equilibrium and mass balance. A geometric scale factor, λ_L, was defined as the proportionality constant between the model and prototype geometry. The geometric scaling factor λ_L used in the present study is 10. The slope height of 0.6 m used in the study in order to simulate a 6 m high prototype slope in
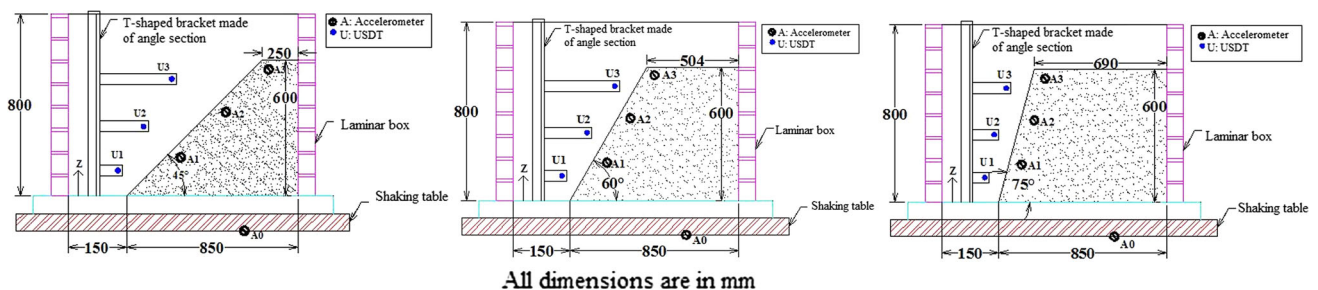

Fig. 3 Schematic diagram of typical slopes with instrumentation

Table 3 Laws of similitude of the prototype and model (as per Iai [33])

Parameter	Model parameter	Equation for scaling factor = (prototype/model)	Scaling factor	Prototype parameter
Acceleration (g)	0.1, 0.2, 0.3	1	1	0.1, 0.2, 0.3
Dimensions of the slope (L × B × H) m	0.85 × 0.5 × 0.6	λ_L	10	8.5 × 5×6
Unit weight of Soil (kN/m³)	15	1	1	15
Frequency (Hz)	f_m	$1/(\lambda_L)^{3/4}$	0.17	$0.17 \times f_m$
Stress	σ_m	λ_L	10	$10 \times \sigma_m$
Time	t_m	$\lambda_L^{3/4}$	5.62	$5.62 \times t_m$
Displacement (m)	d_m	λ_L	10	$10 \times d_m$
Geogrid stiffness at 5% strain (kN/m)	125	λ_L^2	100	12,500

the field. Accordingly the scaling parameters between prototype and model slope were derived are listed in Table 3. Geogrid stiffness at 5% strain is 125 kN/m, which represents a strong prototype geogrid with stiffness 12,500 kN/m in field (Burd and Brocklehurst [34]).

Twenty five different shaking table tests on unreinforced and reinforced soil slope models with slope angles 45°, 60° and 75° were performed in this study. These tests are devised to understand the effect of slope angle on acceleration, frequency of base shaking and reinforcement on the response of the slope during seismic excitation. The test parameters varied in different tests are given in Table 4. The base acceleration was varied from 0.1 to 0.3 g and frequency was varied from 2 to 10 Hz for different tests. Test code for each test gives the slope angle used for constructing the model, number of reinforcing layers, base acceleration and shaking frequency in sequence. Slope angles 45°, 60° and 75° are represented with numerals 45, 60 and 75, respectively. Unreinforced and geogrid reinforced model tests are represented with letter symbols U and G. In case of tests on geogrid reinforced models, the number of geogrid layers used in the model follows the letter G. Base accelerations used were 0.1, 0.2 and 0.3 g in different tests, which are represented as A1, A2 and A3, respectively. Various shaking frequencies used in the tests were 2, 5, 7 and 10 Hz, which were represented by F2, F5, F7 and F10, respectively in the test code. For example, 45G3A3F2 represents the model test, where the slope angle was 45, reinforced with 3 layers of geogrid, subjected to base shaking at an acceleration of 0.3 g and frequency of 2 Hz. The resonant frequencies of the slopes change significantly with the height of the slope. For the model slopes used in this study, shear wave velocity and resonant frequency were calculated as 76 m/s and 32 Hz, respectively as per the equations provided by Hardin and Richart [35] and Hatami and Bathurst [36], as described by Srilatha et al. [37] for a different soil slope. The frequency range used in the present study is much less than the natural frequency and hence the models are not subjected to

resonance. Each model slope is subjected to 40 cycles of base shaking with the corresponding frequency. The elevation is normalized with respect to the height of the slope in all the plots. Photograph of model slope of angle 75° with instrumentation are shown in Fig. 4.

Response of Unreinforced Slopes

Effect of Slope Angle at Different Frequencies

To simplify the presentation of acceleration response at different elevations of the slope, Root mean square acceleration amplification factor (RMSA) is used. RMSA amplification factor is the ratio of response acceleration value in the soil to that of corresponding value of the base motion by Kramer [14]. Acceleration amplification is observed to be the most at the top of the slope in all the tests. These results are similar with those computed by Bathurst et al. [38], Lo Grasso et al. [39].

Figure 5 presents the acceleration response of unreinforced model slopes built to slope angles of 45°, 60° and 75° tested to 40 cycles of base shaking of 0.3 g acceleration and frequency ranging from 2 to 10 Hz. Slight increase in acceleration amplifications was observed with the increase in frequency for all the slopes constructed to different slope angles. Figure 6 presents the horizontal displacements along the height for unreinforced model slopes of different slope angles subjected to four different frequencies 2, 5, 7 and 10 Hz, respectively. All model slopes showed highest displacement response at a frequency of 7 Hz, irrespective of their slope angle. Figure 7 presents the summary of the effect of slope angle on the maximum acceleration amplification factors and horizontal displacements of tested unreinforced slopes subjected to different base shaking frequencies. Figure 7a clearly shows that the slope angle did not influence the acceleration amplifications. Acceleration amplifications were between 1 and 1.5 for all the model slopes, the variation mainly due to the

Table 4 Test parameters varied in the present study

S. no.	Test code	Reinforcement	Slope angle (°)	Acceleration (g)	Frequency (Hz)
1	45UA3F2	None	45	0.3	2
2	45UA3F5	None	45	0.3	5
3	45UA3F7	None	45	0.3	7
4	45UA3F10	None	45	0.3	10
5	45G1A3F2	1 layer Geogrid	45	0.3	2
6	45G2A3F2	2 layer Geogrid	45	0.3	2
7	45G3A3F2	3 layer Geogrid	45	0.3	2
8	45UA1F2	None	45	0.1	2
9	45UA2F2	None	45	0.2	2
10	60UA3F2	None	60	0.3	2
11	60UA3F5	None	60	0.3	5
12	60UA3F7	None	60	0.3	7
13	60UA3F10	None	60	0.3	10
14	60G1A3F2	1 layer Geogrid	60	0.3	2
15	60G2A3F2	2 layer Geogrid	60	0.3	2
16	60G3A3F2	3 layer Geogrid	60	0.3	2
17	60UA1F2	None	60	0.1	2
18	60UA2F2	None	60	0.2	2
19	75UA3F2	None	75	0.3	2
20	75UA3F5	None	75	0.3	5
21	75UA3F7	None	75	0.3	7
22	75UA3F10	None	75	0.3	10
23	75G1A3F2	1 layer Geogrid	75	0.3	2
24	75G2A3F2	2 layer Geogrid	75	0.3	2
25	75G3A3F2	3 layer Geogrid	75	0.3	2

Fig. 4 Photograph of model slope of 75° with instrumentation

change in frequency rather than the change in slope angle. At any specific frequency, model slopes of different slope angles showed almost same acceleration, indicating that the effect of slope angle on the acceleration amplifications is quite minimal. However, Fig. 7b shows the importance of slope angle on the seismic displacements of the slopes. With the increase in slope angle, horizontal displacements increased, irrespective of the shaking frequency. Maximum displacements were observed when the frequency of shaking was 7 Hz for all the cases. A 15° increase in slope angle, from 45° to 60° or from 60° to 75°, caused the maximum deformations increased by about 1.7 times.

Effect of Slope Angle at Different Base Accelerations

To understand the influence of slope angle on the seismic response of slopes at different accelerations of shaking, unreinforced model slopes constructed to angles of 45° and 60° were subjected to 40 cycles of ground shaking at 0.1, 0.2 and 0.3 g accelerations and 2 Hz frequency.

Figures 8 and 9 shows the effect of slope angle on the acceleration and displacement response of unreinforced soil slopes constructed to two different slope angles 45° and 60° at three different shaking accelerations adopted in tests. As observed from Fig. 8, acceleration amplifications are slightly more with the increase in the slope angle. This
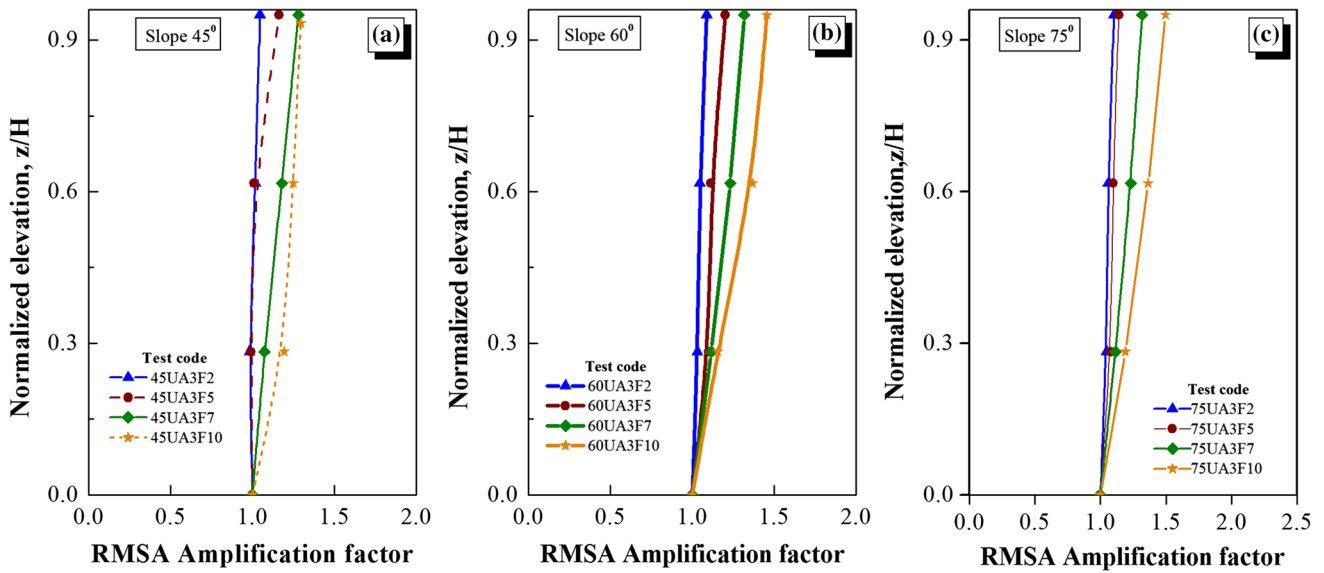
Fig. 5 Acceleration response of unreinforced soil slopes built to different angles. **a** Slope of angle 45°, **b** slope of angle 60° and **c** slope of angle 75°
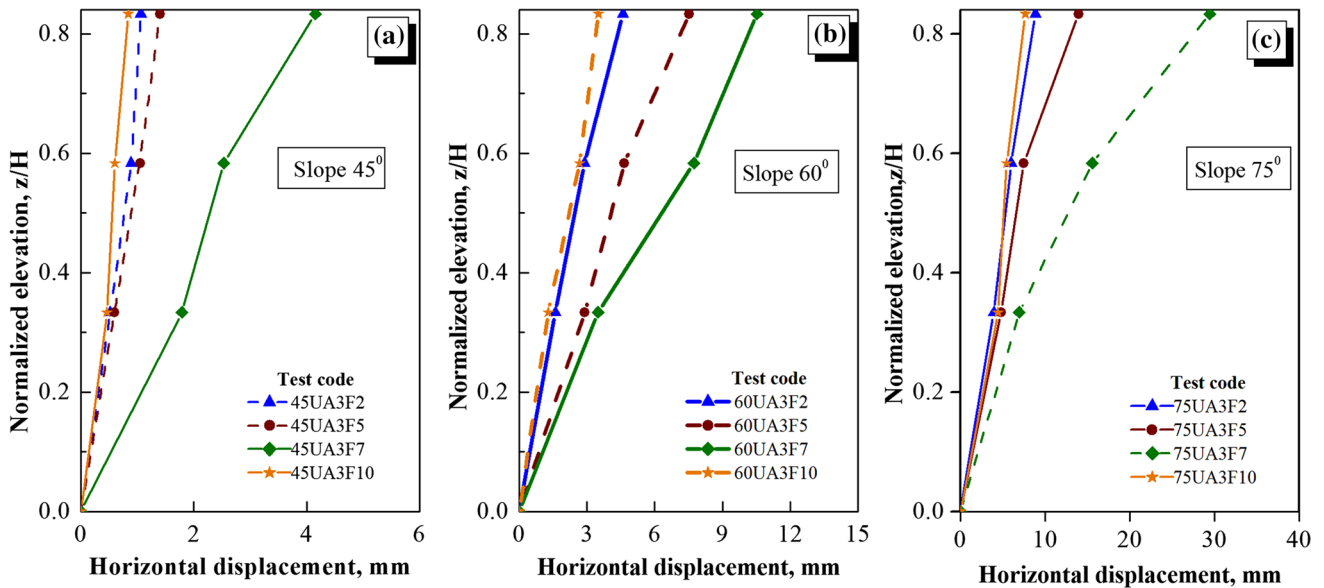

Fig. 6 Horizontal displacements of unreinforced soil slopes built to different angles. **a** Slope of angle 45°, **b** slope of angle 60° and **c** slope of angle 75°

effect of increase in RMSA amplification factors with steeper slopes was more evident at higher accelerations. From the displacement response of slopes presented in Fig. 9, it can be seen that the maximum horizontal displacement of unreinforced slope of 45° was less than 1 mm at accelerations 0.1 g and also at 0.2 g and it increased to slightly beyond 1 mm when the acceleration was 0.3 g. However, in case of steeper slope of 60°, though the maximum displacement was close to 1 mm at 0.1 and 0.2 g accelerations, it suddenly increased to 4.59 mm when the acceleration was 0.3 g. Hence it is clear that the effect of

base acceleration on the displacement response of slope becomes more significant for steeper slopes. As the slope becomes steeper, the frictional force required to keep the slope mass in its position increases. However, the increased unbalanced force on steeper slopes causes the slope mass to deform from its position easily. Increase in base acceleration adds up to the increase in the unbalanced force responsible for slope deformations.

Figure 10 presents the summary of the effect of slope angle on maximum acceleration amplification factors and maximum horizontal displacements of model slopes

Fig. 7 Effect of slope angle on the response of unreinforced soil slopes at different frequencies. **a** Maximum RMSA amplification factors and **b** maximum horizontal displacements
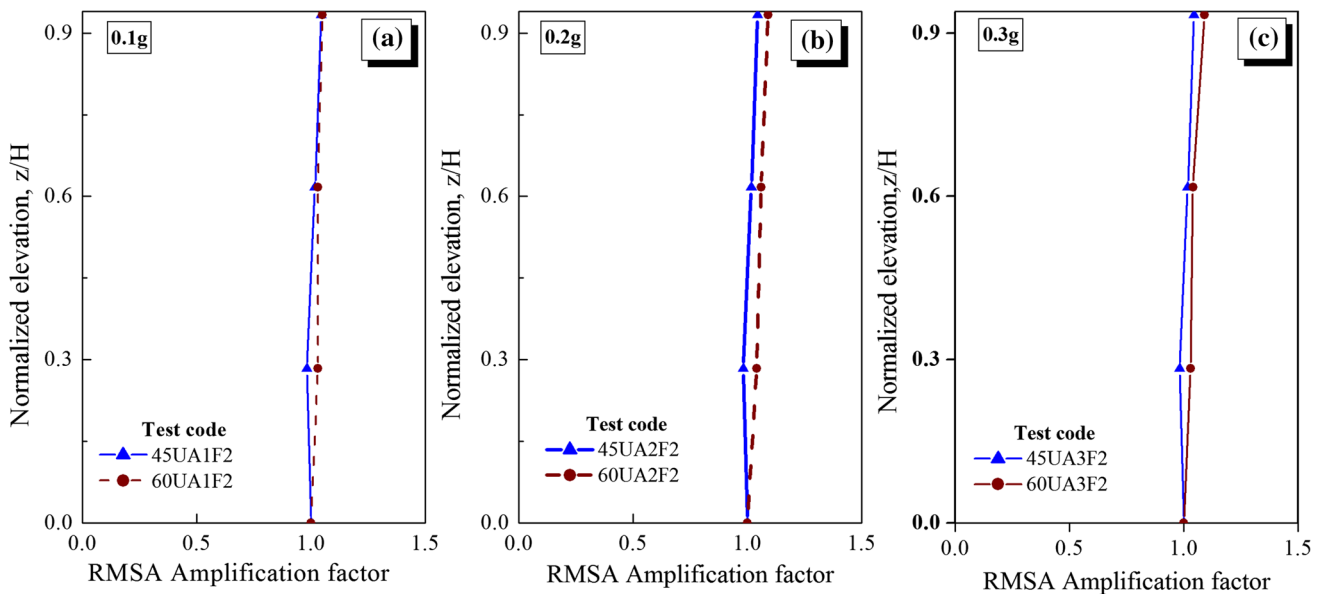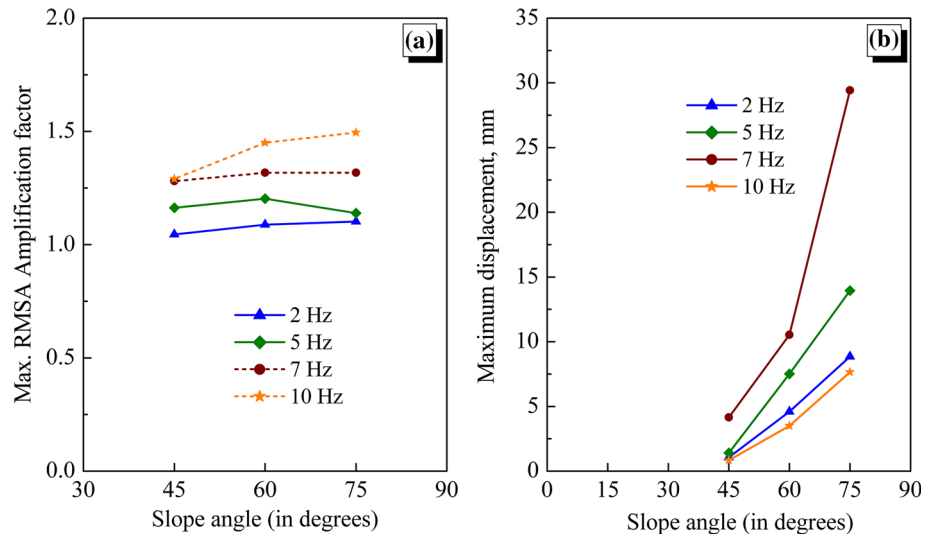

Fig. 8 Acceleration response of unreinforced soil slopes built to different angles tested at different accelerations (2 Hz frequency). **a** 0.1 g, **b** 0.2 g, **c** 0.3 g

subjected to different base accelerations. Slight increase in acceleration amplifications and sudden increase in displacements at higher accelerations can be observed with the increase in the steepness of the slope.

Response of Reinforced Soil Slopes

All these model slopes were subjected to identical base motion of 0.3 g acceleration with shaking frequency of 2 Hz. Figures 11, 12 and 13 presents the effect of slope angle on the acceleration and displacement response of single, two and three layer geogrid reinforced soil slopes,

respectively. RMSA amplification factors computed for slopes of different steepness indicated that increase in the slope angle resulted in slight increase in the acceleration amplification for all reinforced soil slopes. With the increase in the quantity of reinforcement, effect of slope angle on the accelerations increased, as observed from Figs. 11a, 12a and 13a. Soil slopes with larger amount of reinforcement showed higher increase in acceleration amplifications with increase in the slope angle. Horizontal displacements increased with the increase in slope angle at all elevations. The maximum horizontal displacements were 0.84, 3.31 and 6.91 mm for 45°, 60° and 75° model slopes at a normalized height of 0.84 for a single layer
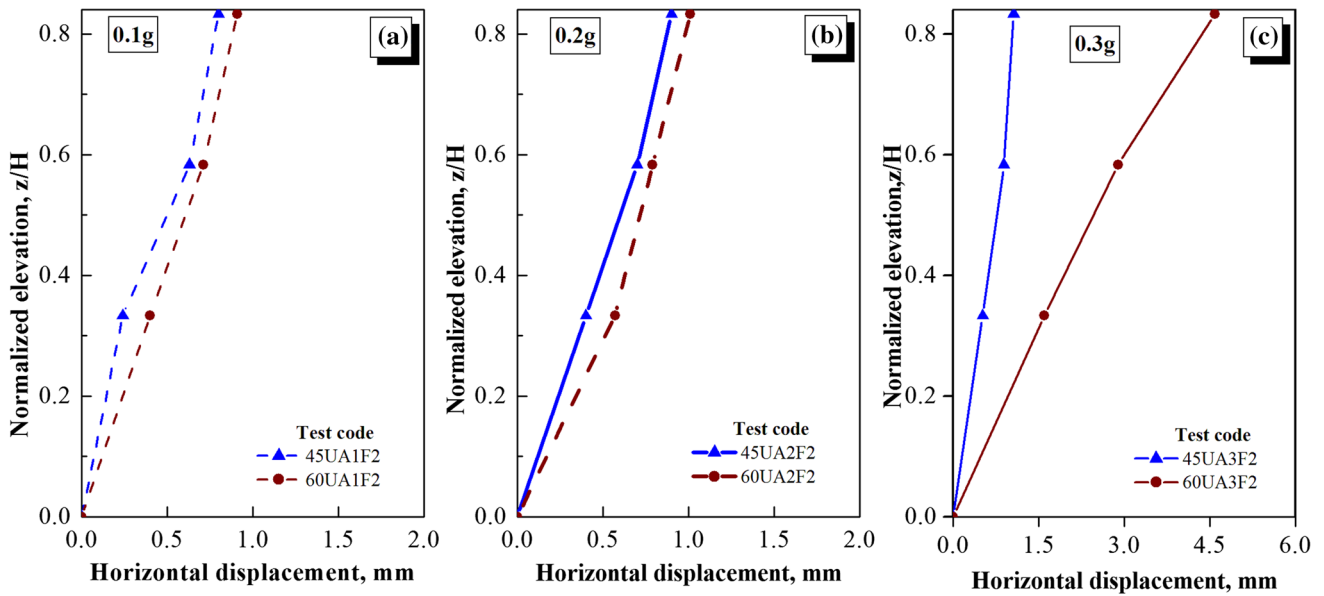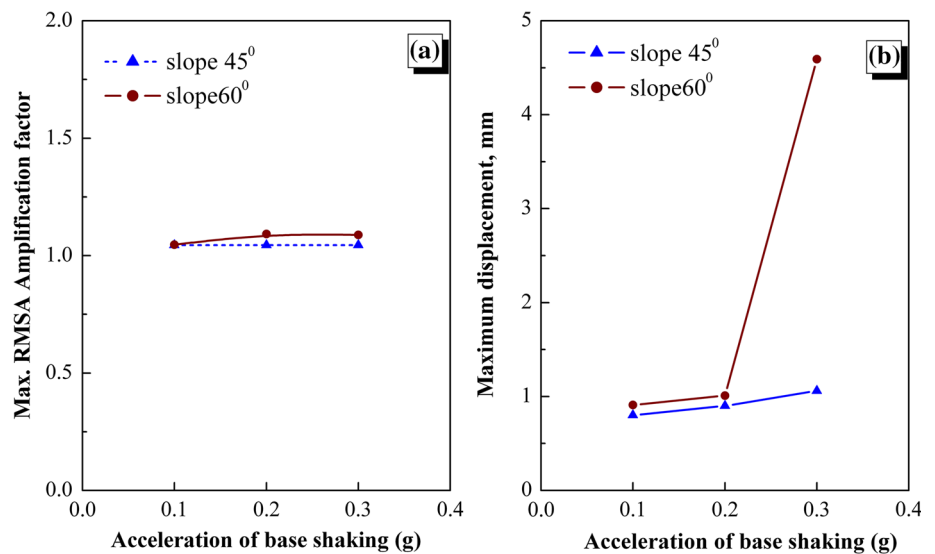
Fig. 9 Displacement response of unreinforced soil slopes built to different angles tested at different accelerations (2 Hz frequency). **a** 0.1 g, **b** 0.2 g, **c** 0.3 g

Fig. 10 Effect of slope angle on the response of unreinforced soil slopes at different base accelerations. **a** Maximum RMSA amplification factors and **b** maximum horizontal displacements

geogrid reinforced slope (Fig. 11b). With the increase in the quantity of reinforcement, the displacements of the slope decreased, but for any specific amount of reinforcement, steeper slopes showed higher displacements. As observed from Fig. 13b, maximum horizontal displacements measured for three layer geogrid reinforced soil slopes were 0.49, 1.60 and 3.67 mm for 45°, 60° and 75° model slopes, respectively at a normalized height of 0.84.

Figure 14 presents the summary of the effect of slope angle on acceleration amplification factors and horizontal displacements of reinforced soil slopes at an acceleration of 0.3 g and frequency of 2 Hz. As observed from Fig. 14a, steeper slopes showed slightly higher acceleration amplifications. More than accelerations, displacements of the slopes were more affected with the slope angle, as shown in Fig. 14b. Substantial increase in the slope deformations was observed with the increase in slope angle of reinforced slopes. However, with the inclusion of reinforcing layers, the deformations were decreased, the decrease being more drastic in case of steeper slopes, as observed by the steep drop the deformations from single layer to three layer reinforcement in case of 75° slope. This result indicates that the reinforcement becomes more effective with the increase in the slope angle in the context of reducing seismic deformations.

Fig. 11 Effect of slope angle on the response of single layer reinforced slopes. a RMSA amplification factors, b horizontal displacements
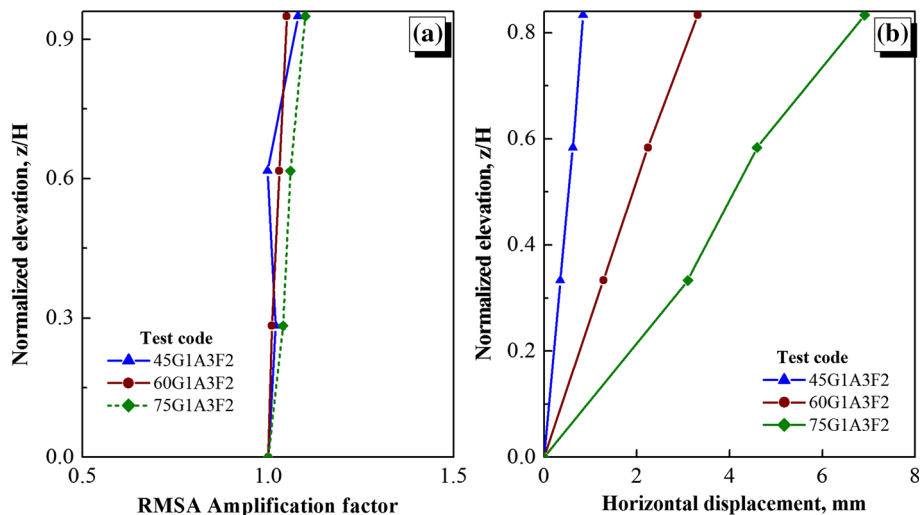

Fig. 12 Effect of slope angle on the response of two layer reinforced slopes. a RMSA amplification factors, b horizontal displacements
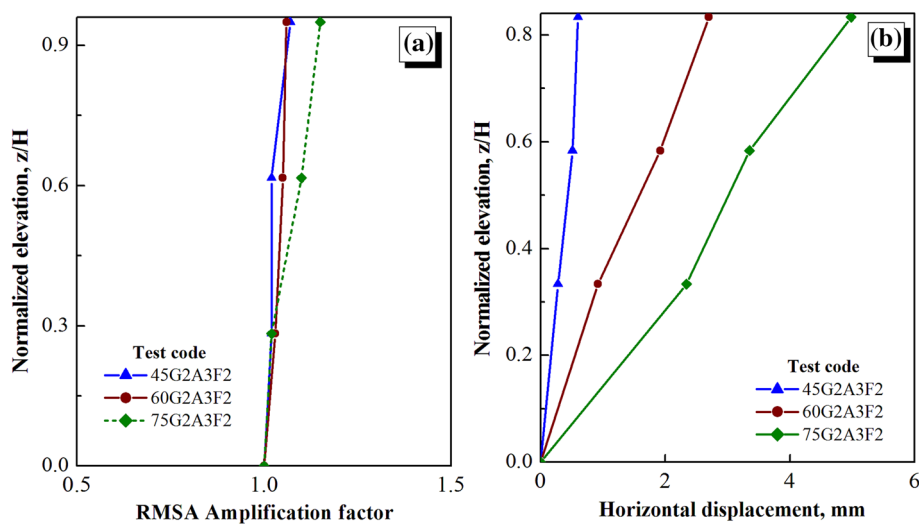

Fig. 13 Effect of slope angle on the response of three layer reinforced slopes. a RMSA amplification factors, b horizontal displacements
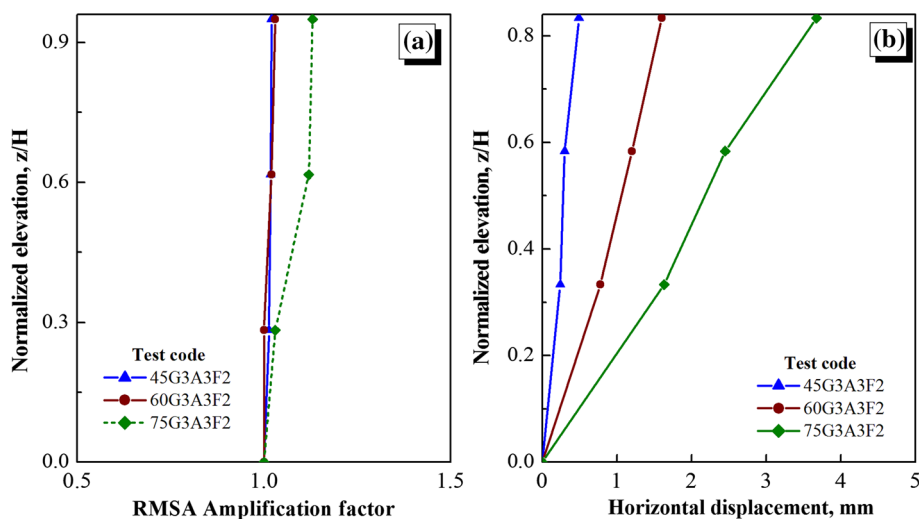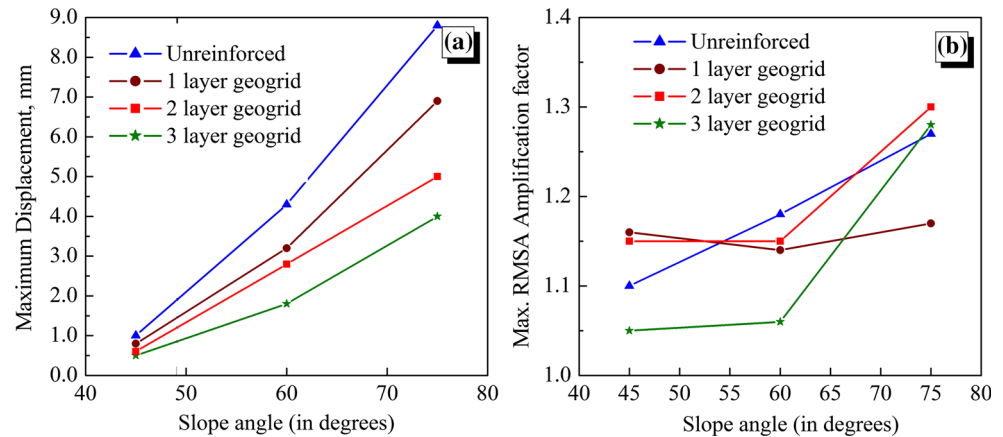
Fig. 14 Effect of slope angle
on the response of reinforced
soil slopes. **a** Maximum RMSA
amplification factors and
b maximum horizontal
displacements

Conclusions

Effect of slope angle on the acceleration and displacement response of unreinforced and reinforced model soil slopes was investigated through shaking table model tests. Unreinforced slopes and slopes reinforced with single, two and three layers of geogrid were constructed to different angles and subjected to different levels of ground shaking conditions to understand the effect of slope angle on their seismic response.

It was observed from the test results that increase in steepness of the slope has detrimental effects on both acceleration amplifications and displacement response of unreinforced as well as reinforced soil slopes. At all frequency and acceleration conditions, unreinforced slopes showed higher amplifications and increased displacements with the increase in steepness. In case of reinforced slopes, the effect of steepness on the acceleration amplifications increased with the quantity of reinforcement. With increased steepness, deformations increased substantially even in case of reinforced soil slopes. Further, the beneficial effect of reinforcement in reducing the horizontal deformations was found to be more pronounced in case of steeper slopes.

References

1. Bonaparte R, Schmertmann GR, Williams ND (1986) Seismic design of slopes reinforced with geogrids and geotextiles. In: Proceedings of the 3rd international conference on geotextiles, Vienna, Austria, vol 1, pp 273–278
2. Ventisette CD, Gigli G, Bonini M, Corti G, Montanari D, Santoro S, Sani F, Fanti R, Casagli N (2015) Insights from analogue modelling into the deformationmechanism of the Vaiont landslide. Geomorphology 228:52–59
3. Koga Y, Matsuo O (1990) Shaking table tests of embankment resting on liquefiable sandy ground. Soils Found 30(4):162–174
4. Perez A (1999) Seismic response of geosynthetic reinforced steep slopes. M.S. thesis, University of Washington, USA
5. Ling HI, Leshchinsky D, Chou NN (2001) Post-earthquake investigation on several geosynthetic-reinforced soil retaining walls and slopes during the Ji–Ji earthquake of Taiwan. Soil Dyn Earthq Eng 21(4):297–313
6. Prasad SK, Towhata I, Chandradhara GP, Nanjundaswamy P (2004) Shaking table tests in earthquake geotechnical engineering. Curr Sci 87(10):1398–1404
7. Lo Grasso AS, Maugeri M, Recalcati P (2005) Seismic behavior of geosynthetic reinforced slopes with overload by shaking table tests. In: Gabr EA, Bowders JJ, Elton D, Zornberg JG (eds) Slopes and retaining structures under static and seismic conditions, ASCE GSP140, pp 1–14
8. Dolce M, Cardone D, Ponzo FC, Valente C (2005) Shaking table tests on reinforced concrete frames without and with passive control systems. Earthq Eng Struct Dyn 34:1687–1717
9. Midorikawa M, Azuhata T, Ishihara WA (2006) Shaking table tests on seismic response of steel braced frames with column uplift. Earthq Eng Struct Dyn 35(14):1767–1785
10. Huang CC, Chen YH (2004) Seismic stability of soil retaining walls situated on slope. J Geotech Geoenviron Eng ASCE 130(1):45–57
11. Huang CC, Horng JC, Chang WJ, Chueh SY, Chiou JS, Chen CH (2010) Dynamic behavior of reinforced slopes: horizontal acceleration response. Geosynth Int 17(4):207–219
12. Huang CC, Horng JC, Chang WJ, Chiou JS, Chen CH (2011) Dynamic behavior of reinforced walls–horizontal displacement response. Geotext Geomembr 29(3):257–267
13. Krishna AM, Latha GM (2007) Seismic response of wrap-faced reinforced soil-retaining wall models using shaking table tests. Geosynth Int 14(6):355–364
14. Latha GM, Krishna AM (2008) Seismic response of reinforced soil retaining wall models: influence of backfill relative density. Geotext Geomembr 26(4):335–349
15. Subermahani M, Ghalandarzadeh A, Fakher A (2009) Experimental study on seismic deformation modes of reinforced-soil walls. Geotext Geomembr 27(2):121–136
16. Srilatha N, Latha GM, Puttappa CG (2013) Effect of frequency on seismic response of reinforced soil slopes in shaking table tests. Geotext Geomembr 36:27–32
17. Varghese RM, Latha GM (2014) Shaking table tests to investigate the influence of various factors on the liquefaction resistance of sands. Nat Hazards 73(3):1337–1351
18. Koga Y, Ito Y, Washida S, Shimazu T (1988) Seismic resistance of reinforced embankment by model shaking table tests. In: Proceedings of international symposium on theory and practice of earth reinforcement, Kukuda, Japan, pp 413–418
19. Kramer SL (2004) Geotechnical earthquake engineering. Prentice Hall, Upper Saddle River

20. Makdisi FI, Seed HB (1978) Simplified procedure for estimating dam and embankment earthquake-induced deformations. J Geotech Eng Div 104(7):849–867

21. Yegian M, Marciano E, Ghahraman V (1991) Seismic risk analysis for earth dams. J Geotech Eng 117(1):18–34

22. Perez A, Holtz R (2004) Seismic response of reinforced steep soil slopes: results of shaking table study. In: Yegian MK, Kavazanjian E (eds) Geotechnical engineering for transportation projects, ASCE GSP 126, Los Angeles, CA, USA, pp 1664–1672

23. Viswanadham BVS, Mahajan R (2007) Centrifuge model tests on geotextile-reinforced slopes. Geosynth Int 14(6):365–379

24. Turan A, Hinchberger SD, El Naggar H (2009) Design and commissioning of a laminar soil container for use on small shaking tables. Soil Dyn Earthq Eng 29:404–414

25. Krishna AM, Latha GM (2009) Seismic behavior of rigid-faced reinforced soil retaining wall models: reinforcement effect. Geosynth Int 16(5):364–3732

26. Ling HI, Leshchinsky D, Wang JP, Rosen A (2009) Seismic response of geocell retaining walls: experimental studies. J Geotech Geoenviron Eng ASCE 135(4):515–524

27. Liu CN, Yang KH, Ho YH, Chang CM (2012) Lessons learned from three failures on a high steep geogrid-reinforced slope. Geotext Geomembr 34:131–143

28. Rajabian A, Viswanadham BVS, Ghiassian H, Salehzadeh H (2012) Centrifuge model studies on anchored geosynthetic slopes for coastal shore Protection. Geotext Geomembr 34:144–157

29. Yang KH, Hung WY, Kencana EY (2013) Acceleration-amplified responses of geosynthetic-reinforced soil structures with a wide range of input ground accelerations. In: Meehan C, Pradel D, Pando MA, Labuz JF (eds) Proceedings of geo congress 2013, California, USA, pp 1178–1187, 3–7 March 2013

30. Latha GM, Varman AMN (2014) Shaking table studies on geosynthetic reinforced soil slopes. Int J Geotech Eng 8(3):299–306

31. Dong H, Ikuo T, Ping QJ, Tetsuya M (2014) Shaking table tests on topographic effects of mountain slopes on their seismic failure. In: International symposium, geohazards: science, engineering and management, Kathmandu, Nepal, pp 348–358, 20–21 November 2014

32. ASTM D 6637 (2001) Standard test method for determining tensile properties of geogrids by the single or multiple-rib tensile method. ASTM standards, West Conshohocken

33. Iai S (1989) Similitude for shaking table test on soil–structure–fluid model in 1 g gravitational field. Soils Found 29(1):105–118

34. Burd HJ, Brocklehurst CJ (1990) Finite element studies of the mechanics of reinforced unpaved roads. In: Proceedings of conference on geotextiles, geomembranes and related products, The Hague, Netherlands, pp 217–221

35. Hardin B, Richart F Jr (1963) Elastic wave velocities in granular soils. J Soil Mech Found Div ASCE 89(1):33–66

36. Hatami K, Bathurst RJ (2000) Effect of structural design on fundamental frequency of reinforced-soil retaining walls. Soil Dyn Earthq Eng 19(3):137–157

37. Srilatha N, Latha GM, Puttappa CG (2016) Seismic response of soil slopes in shaking table tests: effect of type and quantity of reinforcement. Int J Geosynth Ground Eng 2:33

38. Bathurst RJ, Hatami K, Alfaro MC (2002) Geosynthetic reinforced soil walls and slopes: seismic aspects. In: Shukla SK (ed) Geosynthetics and their applications. Thomas Telford, London, pp 327–392

39. Lo Grasso A, Maugeri M, Recalcati P (2004) Shaking table tests and analysis of reinforced slopes. In: Proceedings of 3rd Asian regional conference on geosynthetics, Seoul, Korea, pp 669–676, 21–23 June 2004